

Jet Induced Supernovae: Hydrodynamics and Observational Consequences

A. Khokhlov¹, P. Höflich²

¹ *Naval Research Lab, Washington DC, USA* ² *Department of Astronomy, University of Texas, Austin, TX 78681, USA*

Abstract. Core collapse supernovae (SN) are the final stages of stellar evolution in massive stars during which the central region collapses, forms a neutron star (NS), and the outer layers are ejected. Recent explosion scenarios assumed that the ejection is due to energy deposition by neutrinos into the envelope but detailed models do not produce powerful explosions. There is mounting evidence for an asphericity in the SN which is difficult to explain within this picture. This evidence includes the observed high polarization, pulsar kicks, high velocity iron-group and intermediate-mass elements material observed in remnants, etc.

The discovery of highly magnetars revived the idea that the basic mechanism for the ejection of the envelope is related to a highly focused MHD-jet formed at the NS. Our 3-D hydro simulations of the jet propagation through the star confirmed that the mechanism can explain the asphericities.

In this paper, detailed 3-D models for jet induced explosions of "classical" core collapse supernovae are presented. We demonstrate the influence of the jet properties and of the underlying progenitor structure on the final density and chemical structure. Finally, we discuss the observational consequences, predictions and tests of this scenario.

I INTRODUCTION

Supernovae (SN) are among the most spectacular events because they reach the same brightness as an entire galaxy. This makes them good candidates to determine extragalactic distances and to measure the basic cosmological parameters. Moreover, they are thought to be the major contributors to the chemical enrichment of the interstellar matter with heavy elements. Energy injection by SN into the interstellar medium, triggers star formation and feedback in galaxy formation, and is regarded as a key for our understanding of the formation and evolution of galaxies.

Core collapse supernovae are thought to be the final stages of the evolution of massive stars which live only 10^6 to 2×10^8 years. Such supernovae could be the brightest objects in the distant past when stars first began to form. A

detailed understanding of core collapse is essential to probe the very early phases of the Universe right after the initial star forming period which occurs at redshifts $z \geq 3 \dots 5$. Understanding the mechanism of core collapse supernovae explosions is a problem that has challenged researchers for decades (Hoyle & Fowler 1960). In the general scenario for the explosion, the central region of a massive star collapses and forms a neutron star. Eventually, parts of the potential energy will cause the ejection of the envelope. This general scenario has been confirmed by a wealth of observations including the direct detection of neutrinos in SN1987A and neutron stars in young supernovae remnants.

In recent years, there has been a mounting evidence that the explosions of massive stars (core collapse supernovae) are highly aspherical. (1) The spectra of core-collapse supernovae (e.g., SN87A, SN1993J, SN1994I, SN1999em) are significantly polarized indicating asymmetric envelopes (Méndez et al. 1988; Höflich 1991; Jeffrey 1991; Wang et al. 1996; Wang et al. 2000). The degree of polarization tends to vary inversely with the mass of the hydrogen envelope, being maximum for Type Ib/c events with no hydrogen (Wang et al. 1999, Wang et al. 2000). For supernovae with a good time and wavelength coverage the orientation of the polarization vector tends to stay constant both in time and in the wavelength. This suggests that there is a global symmetry axis in the ejecta (Wang et al. 2000). (2) Observations of SN 1987A showed that radioactive material was brought to the hydrogen rich layers of the ejecta very quickly during the explosion (Lucy 1988; Tueller et al. 1991). (3) The remnant of the Cas A supernova shows rapidly moving oxygen-rich matter outside the nominal boundary of the remnant and evidence for two oppositely directed jets of high-velocity material (Fesen & Gundersen 1997). (4). Recent X-ray observations with the CHANDRA satellite have shown an unusual distribution of iron and silicon group elements with large scale asymmetries in Cas A (Huges et al. 2000). (5) After the explosion, neutron stars are observed with high velocities, up to 1000 km/s (Strom et al. 1995).

There is a general agreement that the explosion of a massive star is caused by the collapse of its central parts into a neutron star or, for massive progenitors, into a black hole. The mechanism of the energy deposition into the envelope is still debated. The process likely involves the bounce and the formation of the prompt shock (e.g. Van Riper 1978, Hillebrandt 1982), radiation of the energy in the form of neutrino (e.g. Bowers & Wilson 1982) and the interaction of the neutrino with the material of the envelope and various types of convective motions (e.g. Herant et al. 1994, Burrows et al. 1995, Müller & Janka 1997, Janka & Müller 1996), rotation (e.g. LeBlanc & Wilson 1970, Saenz & Shapiro S.L. 1981, Mönchmeyer et al. 1991) and magnetic fields (e.g. LeBlanc & Wilson 1970, Bisnovati-Kogan 1971).

Spherically symmetric explosion models rely on the neutrino deposition mechanism. The results depend critically on the progenitor structure, equation of state, neutrino physics, and implementation of the neutrino transport. Currently, results are inconclusive even when using sophisticated Boltzman solvers for the neutrino transport. For example, Mezzacappa et al. (2000) find an explosion whereas

Yamada et al. (1999) and Rammp & Janka (2000) do not. Even if successful, these models cannot explain the observed asymmetries. Within the spherical core-collapse picture, additional mechanisms must be invoked which operate within the envelope itself.

Two such mechanisms have been studied in some detail. One is the Rayleigh-Taylor instability which causes mixing of the layers of different composition when the outgoing shock front passes through (Müller et al. 1989, Benz & Thielemann 1990, Fryxell et al. 1991). This effect can explain mixing of the carbon, oxygen and helium-rich layers required for the SN1987A, but none of the simulations were able to account for the high velocity of Ni observed in SN1987A (Kifonidis et al. 2000). Rayleigh-Taylor mixing provides a rather small-scale structures and can hardly account for the observed polarization which requires a global asymmetry of the expanding envelope (Höflich 1991). Another mechanism involves an explosion inside a rapidly and differentially rotating supernova progenitor (Steinmetz & Höflich 1992). With this mechanism it was possible to account for the polarization in SN1987A which originated from a blue supergiant. This mechanism may have difficulty accounting for the early polarization in some Type II supernovae (Wang et al. 2000) whose light curves indicate a red-giant progenitors. A strong differential rotation in red supergiants can hardly be expected due to their convective envelopes (Steinmetz & Höflich, 1991).

Attempts have also been made to include multi-dimensional effects into a model of collapse itself. The collapsing core becomes unstable due to the gradients of both electron mole fraction Y_e and entropy. The developing convection then affects both the neutrino flux and the energy deposition behind the stalled shock. Numerous studies have demonstrated the presence of this effect. It is still debated whether convection combined with the neutrino transport provides the solution to the supernova problem (Rammp et al. 1998 and references therein). In the current calculations, the size and scale of the convective motions seem to be too small to explain the observed asymmetries. The angular variability of the neutrino flux caused by the convection has been invoked to explain the neutron star kicks (Burrows et al. 1995, Janka & Müller 1994). Calculations give kick velocity up to $\simeq 100$ km/s whereas NS with velocities of several 100 km/s are common.

Rotation of the collapsing core may also be important. It tends to facilitate the explosion because the centrifugal barrier reduces the effective potential for the material moving in the equatorial plane and introduces an axial symmetry in the fluid motions. Simulations made so far indicate that the rotation alone has no or has only a weak effect on the explosion (e.g. Mönchmeyer et al. 1991, Zwerger & Müller 1997). In the latter case it induces a rather weak asymmetry of the explosion with more energy going along the rotational axis.

It has long been suggested that the magnetic field can play an important role in the explosion (LeBlanc & Wilson 1970; Ostriker & Gunn 1971, Bisnovati-Kogan 1971, Symbalisty 1984). LeBlanc and Wilson simulations showed the amplification of the magnetic field due to rotation and the formation of two oppositely directed, high-density, supersonic jets of material emanating from the collapsed core. Their

simulations assumed a rather high initial magnetic field $\sim 10^{11}$ Gauss and produced a very strong final fields of the order of $\sim 10^{15}$ Gauss which seemed to be unreasonable at the time. The recent discovery of pulsars with very high magnetic fields (Kouveliotou et al. 1998, Duncan & Thomson 1992) revives the interest in the role of rotating magnetized neutron stars in the explosion mechanism. It is not clear whether a high initial magnetic field required for the LeBlanc & Wilson mechanism is realistic. On the other hand it may not be needed. Recently Mayer and Wilson (2000, private communication) have suggested that the field amplification and the generation of the jet may continue during the first few seconds of the cooling of the neutron star when the neutron star shrinks rapidly. The current picture of the core collapse process is unsettled. A quantitative model of the core collapse must eventually include all the elements mentioned above.

Due to the difficulty of modeling core collapse from first principles, a very different line of attack on the explosion problem has been used extensively and proved to be successful in understanding of the supernova problem, SN1987A in particular (Arnett et al. 1990, Hillebrand & Höflich 1991). The difference of characteristic time scales of the core (a second or less) and the envelope (hours to days) allows one to divide the explosion problem into two largely independent parts - the core collapse and the ejection of the envelope. By assuming the characteristics of the energy deposition into the envelope during the core collapse, the response of the envelope can be calculated. Thus, one can study the observational consequences of the explosion and deduce characteristics of the core collapse and the progenitor structure. This approach has been extensively applied in the framework of the 1D spherically symmetric formulation. The major factors influencing the outcome have been found to be the explosion energy and the progenitor structure. The same approach can be applied in multi-dimensions to investigate the effects of asymmetric explosions. In this paper we study the effects and observational consequences of an asymmetric, jet-like deposition of energy inside the envelope of a core-collapse supernova.

II NUMERICAL METHODS AND MODEL SETUP

3-D Hydrodynamics: The explosion and jet propagation are calculated by a full 3-D code within a cubic domain of size D . The stellar material is described by the time-dependent, compressible, Euler equations for inviscid flow with an ideal gas equation with $\gamma = 5/3$ plus a component due to radiation pressure with $\gamma = 4/3$. The Euler equations are integrated using an explicit, second-order accurate, Godunov type, adaptive-mesh-refinement, massively parallel, Fully-Threaded Tree (FTT) program, ALLA (Khokhlov 1998). Euler fluxes are evaluated by solving a Riemann problem at cell interfaces. FTT discretization of the computational domain allows the mesh to be dynamically refined or coarsened at the level of individual cells. For more details, see Khokhlov (1998) and Khokhlov et al. (1999ab).

1-D Radiation-Hydrodynamics: About 1000 seconds after the core collapse

and in case of the explosion of red supergiants, the propagation of the shock front becomes almost spherical (see below). To be able to follow the development up to the phase of homologous expansion ($\approx 3 - 5$ days), the 3-D structure is remapped on a 1-D grid, and the further evolution is calculated using a one-dimensional radiation-hydro code (e.g. Höflich et al. 1998) that solves the hydrodynamical equations explicitly in the comoving frame by the piecewise parabolic method (Colella and Woodward 1984).

Radiation Transport: Detailed polarization and flux spectra for asymmetric explosions are calculated using our Monte Carlo code including detailed equations of state. For details, see Höflich (1995), Höflich et al. (1995) & Wang et al. (1998).

The Setup: The computational domain is a cube of size L with a spherical star of radius R_{star} and mass M_{star} placed in the center. The innermost part with mass $M_{\text{core}} \simeq 1.6M_{\odot}$ and radius $R_{\text{core}} = 4.5 \times 10^8$ cm, consisting of Fe and Si, is assumed to have collapsed on a timescale much faster than the outer, lower-density material. It is removed and replaced by a point gravitational source with mass M_{core} representing the newly formed neutron star. The remaining mass of the envelope M_{env} is mapped onto the computational domain. At two polar locations where the jets are initiated at R_{core} , we impose an inflow with velocity v_j ρ_j . At R_{core} , the jet density and pressure are the same as those of the background material. For the first 0.5 s, the jet velocity at R_{core} is kept constant at v_j . After 0.5 s, the velocity of the jets at R_{core} was gradually decreased to zero at approximately 2 s. The total energy of the jets is E_j . These parameters are consistent within, but somewhat less than, those of the LeBlanc-Wilson model.

III RESULTS

A Jet propagation:

As a baseline case, we consider a jet-induced explosion in a helium star. Jet propagation inside the star is shown in Fig. 1. As the jets move outwards, they remain collimated and do not develop much internal structure. A bow shock forms at the head of the jet and spreads in all directions, roughly cylindrically around each jet. The jet-engine has been switched off after about 2.5 seconds the material of the bow shock continues to propagate through the star. The stellar material is shocked by the bow shock. Mach shocks travels two wards the equator resulting in a redistribution of the energy. The opening angle of the jet depends on the ratio between the velocity of the bow shock to the speed of sound. For a given star, this angle determines the efficiency of the deposition of the jet energy into the stellar envelope. Here, the efficiency of the energy deposition is about 40 %, and the final asymmetry of the envelope is about two.

B Influence of the jet properties

Fig. 2 shows two examples of an explosion with with a low and a very high jet velocity compared to the baseline case (Fig. 1). (Fig.1). Fig.2 demonstrates the influence of the jet velocity on the opening angle of the jet and, consequently, on the efficiency of the energy deposition. For the low velocity jet, the jet engine is switched off long before the jet penetrates the stellar envelope. Almost all of the energy of the jet goes into the stellar explosion. On a contrary, the fast jet (61,000 km/sec) triggers only a weak explosion of 0.9 foe although its total energy was $\approx 10\text{foe}$.

C Influence of the progenitor

For a very extended star, as in case of 'normal' Type II Supernovae, the bow shock of a low velocity jet stalls within the envelope, and the entire jet energy is used to trigger the ejection of the stellar envelope. In our example (Fig. 3), the jet material penetrates the helium core at about 100 seconds. After about 250 seconds the material of the jet stalls within the hydrogen rich envelope and after passing about 5 solar masses in the radial mass scale of the spherical progenitor. At this time, the isobars are almost spherical, and an almost spherical shock front travels outwards. Consequently, Strong asphericities are limited to the inner regions. After about 385 seconds, we stopped the 3-D run and remaped the outer layers into 1-D structure, and followed the further evolution in 1-D. After about $1.8\text{E}4$ seconds, the shock front reaches the surface. After about 3 days, the envelope expands homologously. The region where the jet material stalled, expands at velocities of about 4500 km/sec.

Fallback: Jet-induced supernovae have very different characteristics with respect to fallback of material and the innermost structure. In 1-D calculations and for stars with Main Sequence Masses of less than $20 M_{\odot}$ and explosion energies in excess of 1 foe, the fallback of material remains less than $1\text{E-}2$ to $1\text{E-}3 M_{\odot}$ and an inner, low density cavity is formed with an outer edge of ^{56}Ni . For explosion energies between 1 and 2 foe, the outer edge of the cavity expands typically with velocities of about 700 to 1500 km/sec (e.g. Woosley 1997, Höflich et al. 2000). In contrast, we find strong, continuous fallback of $\approx 0.2M_{\odot}$ in the the 3-D hydro models, and no lower limit for the velocity of the expanding material (Fig. 4). This significant amount of fallback must have important consequences for the secondary formation of a black hole. The exact amount and time scales for the final accretion on the neutron star will depend sensitively on the rotation and momentum transport.

Chemical Structure: The final chemical profiles of elements formed during the stellar evolution such as He, C, O and Si are 'butterfly- shaped' whereas the jet material fills an inner, conic structure (Figs. 3 and 5).

The composition of the jets must reflect the composition of the innermost parts of the star, and should contain heavy and intermediate-mass elements, freshly synthesized material such as ^{56}Ni and, maybe, r-process elements because, in our examples, the entropy at the bow shock region of the jet was as high as a few hundred. In any case, during the explosion, the jets bring heavy and intermediate mass elements into the outer H-rich layers.

IV CONCLUSIONS

We have numerically studied the explosion of Core Collapse supernovae caused by supersonic jets generated in the center of the supernova as a result of the core collapse into a neutron star. We simulated the process of the jet propagation through the star, and the redistribution of elements. A strong explosion and a high efficiency for the conversion of the jet energy requires low jet velocities or a low, initial collimation of the jet. With increasing extension of the envelope, the conversion factor increases. Typically, we would expect higher kinetic energies in SNe II compared to SNe Ib/c if a significant amount of explosion energy is carried away by jets. Within the framework of jet-induced SN, the lack of this evidence suggests that the jets have low velocities.

For the compact progenitors of SNe Ib/c, the final departures of the iso-density contours from sphericity are typical a factor of two. This will produce a linear polarization of about 2 to 3 % (Fig. 6) consistent with the values observed for Type Ib/c supernovae. In case of a red supergiant, i.e. SNe II, the asphericity is restricted to the inner few solar masses. In the latter case, the iso-densities show an axis ratios of up to ≈ 1.4 at the innermost, hydrogen-rich layers. The outer layers remain spherical. This has strong consequences for the observations, in particular, for polarization measurements. In general, the polarization should be larger in SNe Ib/c compared to classical SNe II which is consistent with the observations by Wang et al. (2000). Early on, we expect no or little polarization in supernovae with a massive, hydrogen rich envelope which will increase with time to about 1 % (Höflich 1991), depending on the inclination the supernovae is observed. This is also consistent both with the long-term time evolution of SN1987A (e.g. Jefferies 1991) and, in particular, the plateau supernova 1999em which has been observed recently with VLT and Keck (Wang et al. 2000; Leonard et al. 2000).

The He, C, O and Si rich layers of the progenitor show characteristic, butterfly-shape structures. This overall morphology and pattern should be observable in supernovae remnants, e.g. with the Chandra observatory despite some modifications and instabilities when the expanding medium interacts with the interstellar material.

During the explosion, the jets bring heavy and intermediate mass elements into the outer layers including ^{56}Ni . Due to the high entropies of the jet material close to the center, this may be a possible site for r-process elements. Spatial distribution of the jet material will influence the properties of a supernova. In our model for

a SN II, the jet material stalled within the expanding envelope corresponding to a velocity of $\approx 4500\text{km/sec}$ during the phase of homologous expansion. In SN1987A, a bump in spectral lines of various elements has been interpreted by material excited by a clump of radioactive ^{56}Ni (Lucy 1988). Within our framework, this bump may be a measure of region where the jet stalled. This could also explain the early appearance of X-rays in SN1987A which requires strong mixing of radioactive material into the hydrogen-rich layers (see above). We note that, if this interpretation is correct, the 'mystery spot' (Nisenson et al. 1988) would be unrelated. In contrast to 1-D simulations, we find in our models strong, continuous fallback over an extended period of time, and a lack of an inner, almost empty cavity. This significant amount of fallback and the consequences for the secondary formation of a black hole shall be noted. Moreover, fallback and the low velocity material may alter the escape probability for γ -rays produced by radioactive decay of ^{56}Ni . In general, the lower escape probability is unimportant for the determination of the total ^{56}Ni production by the late LCs because full thermalization can be assumed in core collapse SN during the first few years. However, in extreme cases such as SN98BW (e.g. Schaefer et al. 1999), only a small fraction of gamma's are trapped. Effects of multi-dimensionality will strongly alter the energy input by radioactive material and disallow a reliable estimate for the total ^{56}Ni mass.

Finally, we want to emphasize the limits of this study and some of the open questions which will be addressed in future. We have assumed that jets are formed in the course of the formation of a neutron star, and have addressed observational consequences and constrains. However, we have not calculated the jet formation, we do not know if they really form, and, if they form, whether they form in all core-collapse supernovae. We cannot claim that the jets are the only mechanism that can explain asphericity in supernovae although we are not aware of the others. Qualitatively, the observational properties of core collapse supernovae are consistent with jet-induced supernovae and support strongly that the explosion mechanism is highly aspherical but no detailed comparison with an individual object has been performed.

Acknowledgments: We want to thank our colleagues for helpful discussions, in particular, E.S. Oran, L. Wang, J.C. Wheeler, Inzu Yi A., C. Mayers, J.C. Wilson, A. Chieffi, M. Limongi, and O. Straniero. This work is supported in part by NASA Grant LSTA-98-022.

REFERENCES

1. Arnett W.D., Bahcall J.N., Kirshner, R.P., Woosley, S.E. 1990, ARAA 27, 62
2. Benz W., Thielemann F.-K. 1990, ApJ 348, 17
3. Bisnovatyi-Kogan 1971, Soviet Astronomy AJ, 14, 652
4. Bowers R.L., Wilson J.R. 1982 ApJS 50, 115
5. Colella, P.; Woodward, P.R. 1984, J.Comp.Phys. 54, 174
6. Duncan, R. C. & Thompson, C. 1992, ApJ, 392, L9

7. Fesen, R. A. & Gunderson, K. S. 1996, *ApJ*, 470, 967
8. Fryxell B., Arnett D., Müller E. 1991, *ApJ* 367, 619
9. Herant M., Benz W., Hix W.R., Fryer C.L., Colgate S.A. 1994, *ApJ* 435, 339
10. Hillebrandt W., Höflich 1991, *Nuclear Physics B* 19, 113
11. Hillebrandt W. 1982, *ApJ* 103, 147
12. Höflich P., Straniero O., Limongi M. Dominguez I. Chieffi A. 2000, 7th TexMex-Conference, eds. W. Lee & S. Torres-Peimbert, UNAM-Publ., in press & *astro-ph/005037*
13. Höflich, P., Wheeler, J. C., and Thielemann, F.K. 1998, *ApJ* 495, 617
14. Höflich, P. 1995, *ApJ* 443, 89
15. Höflich P., Wheeler, J.C., Hines, D., Trammell S. 1995b, *ApJ* 459, 307
16. Höflich, P. 1991 *A&A* 246, 481
17. Hoyle F., Fowler W. A. 1960, *ApJ* 132, 565
18. Huges J.P., Rakowski C.E., Burrows D.N., Slane P.O. 2000, *AJ*, in press & *astro-ph/9910474*
19. Janka H.T. & Müller E., 1994 *A&A* 290, 496
20. Jeffrey D.J., 1991, *ApJ*, 375, 264
21. Kifonidis K., Plewa T., Janka H.T., Müller E. 2000, *ApJ* 531, 123
22. Khokhlov, A.M., Oran, E.S. 2000, *Combustion & Flame*, in press.
23. Khokhlov A., Höflich P., Oran E.S., Wheeler J.C., P. Wang L., 1999, *ApJ* 524, L107
24. Khokhlov, A.M., Oran, E.S., Chtchelkanova, A.Yu., Wheeler, J.C. 1999a, *Combustion & Flame*, 117, 99
25. Khokhlov, A.M., Oran, E.S., Thomas, G.O., 1999b, *Combustion & Flame*, 117, 323
26. Khokhlov, A.M. 1998, *J.Comput.Phys.*, 143, 519
27. Kouveliotou, C., Strohmayer, T., Hurley, K., Van Paradijs, J., Finger, M. H., Dieters, S., Woods, P., Thompson, C. & Duncan, R. C. 1998, *ApJ*, 510, 115
28. Lucy L.B. 1988, *Proc. of the 4th George Mason conference*, ed. by M. Kafatos, Cambridge University Press, p. 323
29. LeBlanc, J. M. & Wilson, J. R. 1970, *ApJ*, 161, 541
30. Leonard D.C., Filippenko, A.V., Barth A.J., Matheson T. 2000, *ApJ* 536, 239
31. Mezzacappa A., Liebendoerfer M., Bronson Messer O.E. Hix R., Thielemann F-K, Bruenn S.W. 2000, *Phy.Rev.Let.*, accepted
32. Mönchmeyer R., Schaefer G., Mueller E., Kates R.E. 1991 *A&A* 246, 417
33. Müller E., Janka H.T. 1997, *A&A* 317, 140
34. Müller E., Hillebrandt W., Orio M., Höflich P., Mönchmeyer R., Fryxell B.A. 1989, *A&A* 220, 167
35. Nisenson P., Papaliolios C., Karovska M., Noyes R. 1988, *ApJ* 324, 35
36. Ostriker, J. P. & Gunn, J. E. 1971, *ApJ*, 164, L95
37. Rammamp M., Müller E., Ruffert M. 1998, *A&A* 332, 969
38. Rammamp M. and Janka, H.-T. 2000, *ApJ* 593, L33
39. Schaefer B. 2000, *ApJ* 533, 21
40. Saenz R.A., Shapiro S.L. 1981, *ApJ* 244, 1033
41. Steinmetz M., Höflich P. 1992, *A&A* 257, 641
42. Symbalisky E.M.D. 1984, *ApJ* 285, 729
43. Straniero, O. Chieffi, A. and Limongi M. 1999 *ApJ*, in press

44. Strom R., Johnston H.M., Verbunt F., Aschenbach B. 1995, *Nature*, 373, 587
45. Symbalisy E.M.D. 1984, *ApJ* 285, 729
46. Trammell S., Hines D., Wheeler J.C. 1993, *ApJ* 414, 21
47. Tueller J., Barthelmy S., Gehrels N., Leventhal M., MacCallum C.J., Teegarden B.J. 1991, in: *Supernovae*, ed. S.E. Woosley, Springer Press, p. 278
48. Van Riper K.A. 1978, *ApJ* 221, 304
49. Wang L., Howell A., Höflich P., Wheeler J.C. 2000, *ApJ*, in press
50. Wang, L., Wheeler, J. C., Li, Z. W., & Clocchiatti, A. 1996, *ApJ*, 467, 435
51. Wang, L., Wheeler, J.C., Höflich, P. 1997, *ApJ*, 476, 27
52. Yamada S., Janka H.T., Suzuki H. 1999, *A&A* 344, 533
53. Zwerger T., Müller E. 1997, *A&A* 320, 209

FIGURE 1. Logarithm of the density structure as a function of time for a helium core. The total mass of the ejecta is $2.6 M_{\odot}$. The initial radius, velocity and density of the jet were taken to 1200 km 32,000 km/sec and $6.5E5g/cm^3$, respectively. The shown domains 7.9, 9.0, 36 and $45 \times 10^9 cm$. The total energy is about 9E50 erg. After about 4.5 seconds, the jet penetrates the star. The energy deposited in the stellar envelope by the jet is about 4E50 erg, and the final asymmetry is of the order of two.

FIGURE 2. Same as Fig. 1 ($0.5 \leq \log(\rho) \leq 5.7$) but for a jet velocity of 61,000 km/sec and a total energy of 10 foe at $\approx 1.9sec$ (left), and 11,000 km/sec and a total energy of 0.6 foe (right). The size of the presented domains are 5 (left) and $2 \times 10^{10}cm$ (right), respectively. For the high velocity jet, most of the energy is carried away by the jet. Only 0.9 foe are deposited in the expanding envelope. In case of a low velocity jet, the bow-shock still propagates through the star after the jet is switched off (at $\approx 3sec$), and the entire jet energy is deposited in the expanding envelope.

FIGURE 3. Same as Fig. 1 but helium abundance (between 0 to 1) for the explosion of a red supergiant with $207 R_{\odot}$ and $7.6 M_{\odot}$. The jet velocity of 11,000 km/sec and a total energy of 2 foe has been taken. A domain of about $1.4 \times 10^{12}cm$ is shown. After about 30 seconds, the material of the bow shock penetrates the Helium core, and, at about 250 seconds, the jet material 'stalls' in the hydrogen rich layers. Subsequently a almost spherical shock front propagates through the star. In the final configuration, asymmetries are restricted to the layers within the 2 to 3 solar masses of the h-rich envelope. After homologous expansion, the region corresponding to the stalled shock expands with about 4000 km/sec. All of the jet energy is deposited in the expanding envelope.

FIGURE 4. Same as Fig. 3 but the velocity distribution in the xy- and yz plane for the very inner regions at about 250 sec. Note the qualitative difference between 1-D and multidimensional results. In 1-D, a large, almost empty cavity is found with expansion velocities of a about 4000 km/sec for corresponding explosions. In multidimensional simulations shown here, this cavity is all but absent. Still, after in multidimensional simulations material can be found up with low velocities. Even infall can persist over a rather extended period of time.

FIGURE 5. Same as Fig. 3 but the distribution of O and the jet material

FIGURE 6. Polarization spectrum for SN1993J for an axis ratio of 1/2 for an oblate ellipsoide in comparison with observations by Trammell et al. (1993) are given in the left plot. On the right, the dependence of the continuum polarization (right) and directional dependence of the luminosity is shown as a function axis ratios for oblate ellipsoids seen from the equator (from Höflich, 1991 & Höflich et al. 1995b).

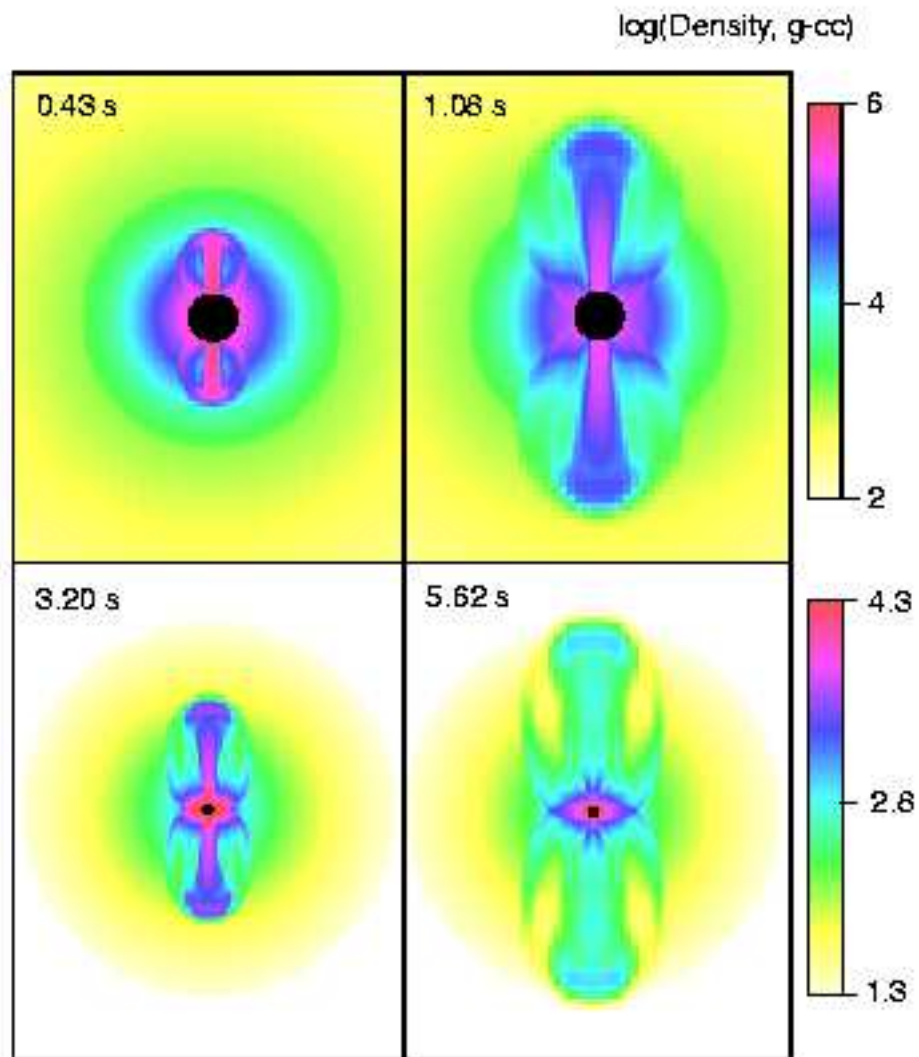


FIGURE 1. Logarithm of the density structure as a function of time for a helium core. The total mass of the ejecta is $2.6 M_{\odot}$. The initial radius, velocity and density of the jet were taken to 1200 km 32,000 km/sec and $6.5E5 \text{ g/cm}^3$, respectively. The shown domains 7.9, 9.0, 36 and $45 \times 10^9 \text{ cm}$. The total energy is about 9E50 erg. After about 4.5 seconds, the jet penetrates the star. The energy deposited in the stellar envelope by the jet is about 4E50 erg, and the final asymmetry is of the order of two.

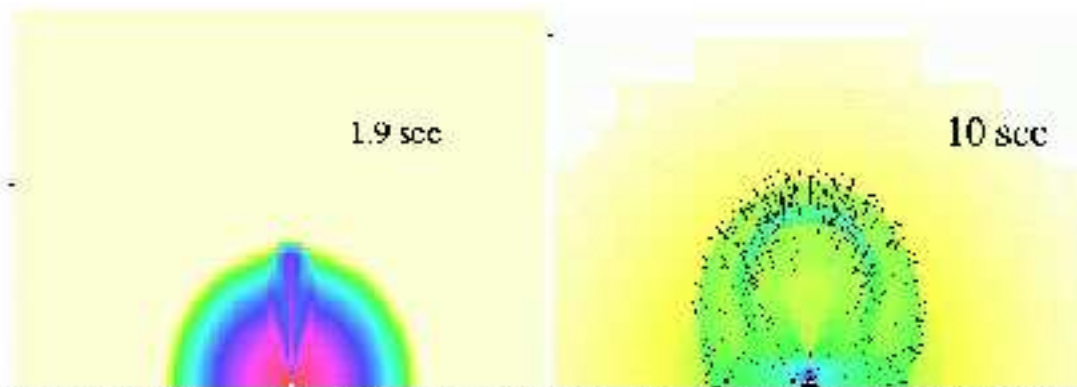


FIGURE 2. Same as Fig. 1 ($0.5 \leq \log(\rho) \leq 5.7$) but for a jet velocity of 61,000 km/sec and a total energy of 10 foe at ≈ 1.9 sec (left), and 11,000 km/sec and a total energy of 0.6 foe (right). The size of the presented domains are δ (left) and $2 \cdot 10^{10}$ cm (right), respectively. For the high velocity jet, most of the energy is carried away by the jet. Only 0.9 foe are deposited in the expanding envelope. In case of a low velocity jet, the bow-shock still propagates through the star after the jet is switched off (at ≈ 3 sec), and the entire jet energy is deposited in the expanding envelope.

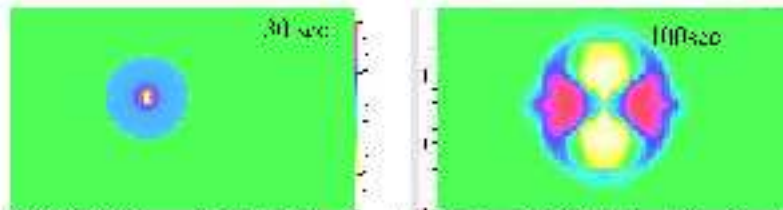


FIGURE 3. Same as Fig. 1 but helium abundance (between 0 to 1) for the explosion of a red supergiant with $20 M_{\odot}$ and $2.8 M_{\odot}$. The jet velocity of $11,000 \text{ km/sec}$ and total energy of 2 has been taken. A domain of about $1.4 \times 10^{16} \text{ cm}$ is shown. After about 30 seconds, the material of the low shock penetrates the Helium core, and, at about 200 seconds, the jet material 'fills' in the hydrogen rich layers. Subsequently a almost spherical shock front propagates through the star. In the final configuration, symmetries are restricted to the layers within the 2 to 3 substructure of the h-rich envelope. After homologous expansion, the region corresponding to the shell shock expands with about 4000 km/sec . All of the jet energy is deposited in the expanding envelope.

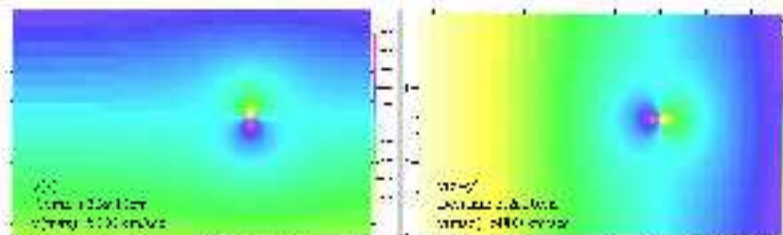


FIGURE 4. Same as Fig. 3 but the velocity distribution in the xy - and yz -plane for the very inner regions at about 200 sec. Note the qualitative difference between 1-D and multidimensional results. In 1-D, a large, almost empty cavity is found with expansion velocity of \approx about 4000 km/sec for corresponding explosions. In multidimensional simulations shown here, this cavity is all but absent. Still, after in multidimensional simulations material can be found up with low relative. Even infall can persist over a rather extended period of time.

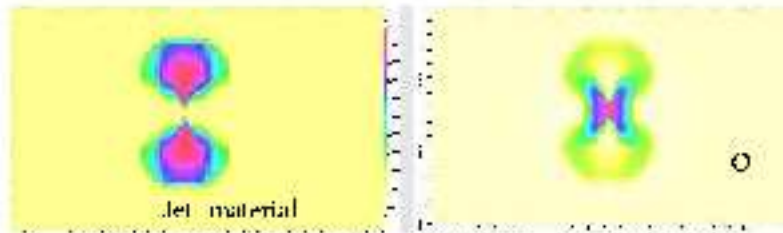


FIGURE 5. Same as Fig. 3 but the distribution of O and the jet material

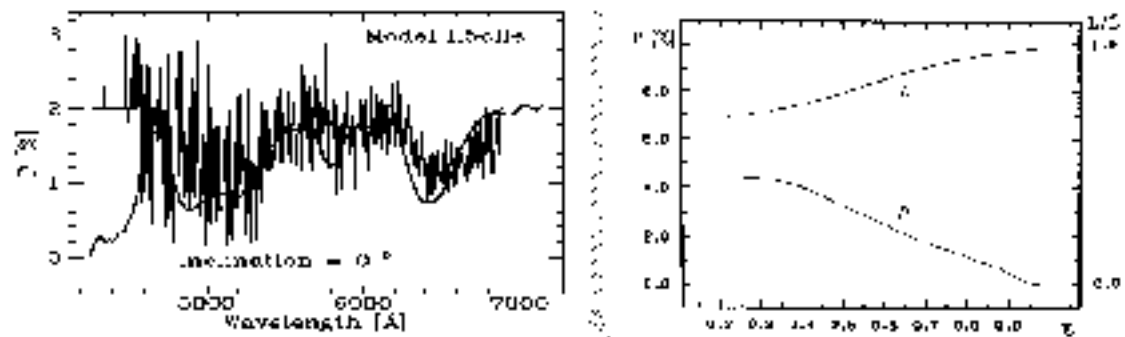


FIGURE 6. Polarization spectrum for SN1993J for an axis ratio of $1/2$ for an oblate ellipsoide in comparison with observations by Trammell et al. (1993) are given in the left plot. On the right, the dependence of the continuum polarization (right) and directional dependence of the luminosity is shown as a function axis ratios for oblate ellipsoide seen from the equator (from Höflich, 1991 & Höflich et al. 1995b).